

# **Ductility and Energy Absorbing Behaviour of Coal Wash – Rubber Crumb Mixtures**

Haydn Hunt<sup>a</sup>, Buddhima Indraratna<sup>a\*</sup>, and Yujie Qi<sup>a</sup>

*<sup>a</sup>Transport Research Centre, School of Civil and Environmental Engineering,  
University of Technology Sydney, Sydney, Australia*

\* Corresponding author

Distinguished Prof. Buddhima Indraratna

Director, Transport Research Centre, University of Technology Sydney

Email: [buddhima.indraratna@uts.edu.au](mailto:buddhima.indraratna@uts.edu.au)

## **Haydn Hunt**

PhD Candidate, School of Civil and Environmental Engineering, University of Technology Sydney, NSW 2007, Australia.

Email: [haydn.r.hunt@student.uts.edu.au](mailto:haydn.r.hunt@student.uts.edu.au)

**Buddhima Indraratna** *PhD (Alberta), MSc (Lond.), BSc (Hons., Lond.), DIC, FTSE, FIEAust., FGS, CEng, CPEng*

Distinguished Professor of Civil Engineering, Founding Director of Australian Research Council's Industrial Transformation Training Centre for Advanced Technologies in Rail Track Infrastructure (ITTC-Rail), Director of Transport Research Centre, School of Civil and Environmental Engineering, University of Technology Sydney, NSW 2007, Australia.

Email: [buddhima.indraratna@uts.edu.au](mailto:buddhima.indraratna@uts.edu.au)

**Yujie Qi** *PhD, MSc, BSc*

Lecturer, and Program Co-leader of Transport Research Centre, School of Civil and Environmental Engineering, University of Technology Sydney, NSW 2007, Australia.

Email: [yujie.qi@uts.edu.au](mailto:yujie.qi@uts.edu.au)

Word count: 7507

# 1 Ductility and Energy Absorbing Behaviour of Coal Wash – Rubber 2 Crumb Mixtures

3 **Abstract:** The reuse of waste materials such as coal wash (CW) and rubber crumbs  
4 (RC) is becoming increasingly popular in large-scale civil engineering  
5 applications, which is environmentally friendly and economically attractive. In this  
6 study, the ductility and strain energy density of CW-RC mixtures with different  
7 RC contents compacted to the same initial void ratio and subjected to triaxial  
8 shearing are evaluated. As expected, the ductility and energy absorbing capacity  
9 of the waste mixture are improved with RC addition. This makes the use of CW-  
10 RC mixtures in substructure applications is a promising development for future rail  
11 design where loads are expected to increase. Furthermore, empirical models for the  
12 shear strength and strain energy density based on the RC content are proposed.  
13 These models may be used as a guide to approximate the shear strength and strain  
14 energy density of these compacted CW-RC mixtures prior to the undertaking of  
15 extensive triaxial tests.

16 **Keywords:** Coal wash; Rubber Crumbs; Ductility; Energy absorbing capacity

## 17 **1. Introduction**

18 Coal wash (CW) is a waste by-product of the coal washing process in mining operations,  
19 with several million tons produced each year in Australia [1]. On the other hand,  
20 approximately 50 million equivalent passenger units (EPU) of rubber tyres (1 EPU  
21 corresponds to a standard 8 kg rubber tyre) reach their end of life in Australia, equating  
22 to about two tyres per capita [2]. These waste materials are becoming an increasing  
23 problem within many developed and industrial countries as they are generally disposed  
24 of in landfills or stockpiled, leading to the occupation of usable land [3]. Non-recycled  
25 scrap tyres can lead to various economical, health and environmental concerns, and fires  
26 in stockpiles of waste tyres can occur due to exothermic reactions of rubber leading to  
27 spontaneous combustion and the release of toxic gases [4–6]. Moreover, measures have  
28 also been put in place with a levy of AUD \$15.00 per tonne of coal washery rejects  
29 received from off-site and applied to land as an economic incentive to develop  
30 alternatives to disposal in Australia [7]. Therefore, it is of great significance to reuse these  
31 waste products in large-scale civil engineering projects as large quantities can be  
32 removed/diverted from stockpiles and landfills, thus reducing the negative health and  
33 environmental impacts as well as the requirement for valuable natural aggregates to be  
34 obtained through quarrying [8,9]. The use of scrap tyres in civil (geotechnical)  
35 engineering applications has been standardised by ASTM [10], where specifications on  
36 aspects such as sizing, material properties, and construction practices are provided.

37 For important structures, a prolonged ductile failure is preferred over a sudden  
38 and brittle one. Railway tracks are no different in this regard as a brittle failure of the  
39 substructure can be catastrophic due to the high train speeds and civilian use. As an  
40 individual material, compacted coal wash has a brittle strain-softening response similar  
41 to a dense sand at relatively low confining pressures ( $\sigma'_3 \leq 50$  kPa) [11]. As a result, it is

42 unlikely to be suitable for substructure use in this aspect. Although, rubber has been  
43 shown to increase the ductility and reduce the stiffness of sand [6,12–15], rubberised  
44 concrete [16–19], and other waste material mixtures [9,20–23], in the long term, the  
45 stiffness of the mixture can increase due to creep deformation, especially when the host  
46 materials are crushable like coal wash [24]. Therefore, the addition of rubber crumbs  
47 (RC), produced by shredding scrap tyres, may enhance the ductile capacity of CW and  
48 render it suitable for track substructure use.

49         The energy absorbing capacity and damping properties of rubber are also ideal for  
50 dynamic applications. Its use in soil mixtures [9,20,22,25,26], and under sleeper pads [27]  
51 has been shown to improve energy dissipation, decrease particle breakage, and reduce  
52 vibration intensity. Enhancing the energy absorption of the subballast layer may help  
53 reduce the energy transferred to the underlying subgrade. This is important as most  
54 coastal regions in Australia have very soft clays with a low bearing capacity and high  
55 compressibility [28] and hence strength and excessive settlements are a major concern  
56 for track design. Furthermore, a compressible and energy absorbing subballast layer can  
57 act as a flexible cushion, helping to reduce breakage of the overlying ballast layer as well.  
58 Overlying a stiffer substructure, ballast subjected to impact loading experienced more  
59 breakage compared to that on top of a more compressible layer [28]. An increased number  
60 of fines from this breakage process can lead to fouling and reduce the stiffness of the  
61 ballast layer, causing potential track instability and degradation. Therefore, the higher  
62 ductility and energy absorbing potential of these recycled waste materials may help  
63 reduce track degradation over time and lead to an overall safer design.

64         This study aims to investigate the influence rubber crumb content has on the  
65 ductility, shear strength and strain energy absorption of a compacted CW-RC matrix.  
66 Furthermore, by comparing the geotechnical properties of the mixtures to that of typical

67 subballast materials, an optimal RC content is proposed. To achieve this, the consolidated  
68 drained monotonic triaxial tests results on CW-RC mixtures with varying RC contents (0,  
69 5, 10, and 15% by weight) tested by Indraratna et al. [20] were adopted in this study. The  
70 test specimen was compacted at a modified energy level in order to reach an initial void  
71 ratio of 0.3 suggested by Australian Rail Track Corporation [29]. The tests were  
72 conducted at a range of relatively low effective confining pressures ( $\sigma'_3 = 10, 25, 50,$  and  
73  $75$  kPa) to simulate the low magnitude of confinement in typical subballast conditions.  
74 The particle size distribution of the CW-RC mixtures is provided in Figure 1. For detailed  
75 specimen preparation and test procedures, see [9,20].

## 76 **2. Ductility of the waste material matrix**

77 The stress-strain curves for the CW-RC mixtures tested at  $\sigma'_3 = 10, 25, 50,$  and  $75$  kPa  
78 are shown in Figure 2. It is to be noted that no tests have been undertaken for 15% RC at  
79  $10$  kPa confining pressure. It can be seen that the peak deviator stress,  $q_{peak}$ , decreases  
80 and the corresponding axial strain ( $\epsilon_1$ ) at  $q_{peak}$  increases with RC contents. This can be  
81 attributed to the lower shear strength and higher compressibility of RC with increased  
82 rubber-to-rubber interactions within the skeleton as RC contents increase [6,22].  
83 Additionally, the curvature of the stress-strain response at the peak becomes broader with  
84 RC addition. In other words, the addition of RC has caused a transition from a  
85 predominately brittle to a more ductile post-peak state for the waste mixture. This  
86 transition is especially important for railway applications as large loads and high speeds  
87 coupled with sudden failure of the track can cause catastrophic train derailments. The  
88 increased ductility means that, although larger settlements are experienced, the  
89 substructure can sustain a larger post-peak load and lower the potential risk of financial  
90 and human loss from derailments.

91 Moreover, all the test specimens achieved the residual state by the end of the test  
92 ( $\varepsilon_1 = 20\%$ ), where the reduction of deviator stress is negligible upon further straining in  
93 the vertical direction. Note that, under a certain  $\sigma'_3$  all the CW-RC mixtures tend to end  
94 up with similar residual state deviator stress ( $q_{residual}$ ), indicating the addition of RC  
95 does not incur a significant impact on the residual strength of the waste mixture.

96 The volume change behaviour for each mixture is also contained in Figure 3. All  
97 specimens exhibited an initial volumetric contraction, with the compressive peak  
98 occurring at a larger axial strain as the rubber content within the mixture increases. Before  
99 the addition of rubber, due to the incompressibility of the CW particles, the optimum  
100 packing arrangement of the skeleton (by particle breakage and rearrangement mostly) is  
101 reached at a much earlier stage of loading and strain. As RC is added and compressed,  
102 further voids/spaces are created for the CW particles to occupy and the optimum packing  
103 arrangement is reached at a later stage. Additionally, at a confining pressure of 50 kPa,  
104 the mixtures with at least 10% RC remained contractive at failure.

105 To evaluate the ductility of the CW-RC mixture, the brittleness index ( $I_B$ ) initially  
106 proposed by Consoli et al. [30] is adopted in this study, which is defined as

$$107 \quad I_B = \frac{q_{peak}}{q_{residual}} - 1 \quad (1)$$

108 where  $q_{peak}$  and  $q_{residual}$  are the peak and residual state deviator stresses, respectively.  
109 The smaller the value of the brittleness index, the greater the ductility of the material.

110 The brittleness indices of the CW-RC mixtures with respect to the RC content and  
111 confining pressure are shown in Figure 4. Generally,  $I_B$  decreases with the increasing RC  
112 content when  $RC \leq 10\%$ , then it increases again as 5% more RC is added. This indicates  
113 that the mixture has the minimum brittle index (i.e., the maximum ductility) when adding  
114 10% RC (Figure 4 (a)). This is because when the mixture skeleton is formed by CW ( $RC \leq$

115 10%), The brittleness is positively correlated to the particle breakage of the materials (i.e.  
116 coal wash in this study) as particle breakage cause the material skeleton to lose its original  
117 structure and deteriorate its stress bearing capacity [31]. By adding rubber, particle  
118 breakage of the CW-RC mixture was reduced significantly (e.g. 18% and 46% reduction  
119 by adding 0% and 10% rubber, respectively) reported by Qi et al. [32], which would have  
120 certainly contributed to the reduction of the brittleness as rubber content increases.  
121 However, when  $RC > 10\%$ , the skeleton of the CW-RC mixtures is pronouncedly  
122 influenced by rubber particles, thus the reduction of particle breakage becomes  
123 insignificant by adding more rubber (only 1% more by increasing rubber content from  
124 10% to 15% [32]). Therefore, no further reduction in brittleness can occur by adding more  
125 rubber. For a CW-RC mixture with a certain RC content,  $I_B$  decreases as the effective  
126 confining pressure increases, albeit fluctuation is observed for the mixture with 5% RC  
127 (Figure 4 (b)). Additionally, when compared to typical subballast, all CW-RC mixtures  
128 are more ductile at lower confining pressures ( $\sigma'_3 \leq 25$  kPa). Mixtures with 10% and 15%  
129 RC are the best performing with lower  $I_B$  indices than the subballast under all confining  
130 pressures tested.

### 131 **3. Shear Resistance**

#### 132 **3.1. Internal friction angle**

133 Several studies on rubber-soil and rubber-waste mixtures [6,9,20,22] have analysed the  
134 peak friction angle with respect to the rubber content. This parameter is indicative of the  
135 shear strength at a certain confining pressure since it is a function of  $\sigma'_3$  and is therefore  
136 an extrinsic material property. The use of a constant and intrinsic friction angle,  $\phi'$ , may  
137 be more beneficial and efficient for use in geotechnical design. Table 1 shows the peak  
138 friction angle and internal frictional angle of the CW-RC mixtures.

139           Figure 5 compares the internal friction angle for the CW-RC mixtures (obtained  
140 using Mohr circles and linear failure envelope for peak stress values) with  $\phi' = 41.6^\circ$  for  
141 typical subballast determined from tests conducted by Qi et al. [22]. It is noteworthy that  
142 when the amount of rubber is more than 10%, the internal friction angle becomes less  
143 than that of traditional subballast, suggesting the CW-RC mixtures should keep the rubber  
144 content  $\leq 10\%$  to ensure a superior shear strength in contrast to conventional subballast.  
145 The Mohr circles and approximated linear failure envelope for the mixture with 10% RC  
146 are contained in Figure 6. It should be stressed that this angle of friction can be simplified  
147 as a constant to fit a linear failure envelope, while for these types of waste materials it is  
148 likely to be non-linear with the variation of  $\sigma'_3$  [20,22,33]. Non-linear failure envelopes  
149 are also observed for CW [34] and sand-rubber mixtures [6,12]. Under lower confining  
150 pressures, and hence normal stresses, the discrepancy between these linear and non-linear  
151 models becomes more noticeable and as such a relatively high cohesion intercept obtained  
152 from a linear model may be misconstrued. A linear Mohr Coulomb frictional model is  
153 better representative of loose soils with loosely packed particle arrangements. As the  
154 rubber content increases so too does the degree of particle packing within the matrix to  
155 comply with the compaction requirements suggested by Australian Rail Track  
156 Corporation [29]. Accordingly, mixtures with higher rubber contents conform less to a  
157 linear failure envelope, especially at lower confining pressures where the influence of  
158 additional particle interlocking resistance is more significant relative to the confinement  
159 provided.

160           Furthermore, as the normal stress increases so too does the particle breakage due  
161 to concentrated stress points between particles within a granular matrix. This reduces the  
162 interlocking forces and hence the envelope diverges from the linear Mohr-Coulomb  
163 model for these higher stresses as well. This is supported by experimental studies on CW

164 [3,34,35,36] where non-linear envelopes are also observed as it is more susceptible to  
165 higher breakage relative to other rigid aggregates, particularly under higher normal  
166 stresses [3,9,11,22,36,37]. Although, as rubber reduces particle breakage due to its energy  
167 absorbing properties, the divergence from a linear envelope is relatively small within the  
168 range of confining pressures tested (Figure 6).

### 169 **3.2. Shear Strength Model**

170 The shear strength,  $\tau_f$ , is obtained corresponding to the peak deviator stress suggested by  
171 Qi et al. [22] for SFS-CW-RC mixtures and Kim and Santamarina [15] for sand-rubber  
172 mixtures as in Equation (2a):

$$173 \quad \tau_f = \frac{q_{peak} \cos \phi'_{peak}}{2} \quad (2a)$$

174 Both linear and non-linear failure envelopes for the CW-RC mixtures with 10% RC are  
175 constructed from the Mohr circles in Figure 6. Although the envelopes are similar for the  
176 range of stresses tested, a linear envelope with a non-zero cohesion intercept may  
177 overestimate the shear strength of the mixtures, particularly at lower confining pressures.  
178 Additionally, as previously discussed, CW exhibits non-linear shear behaviour,  
179 particularly at higher stresses due to the impact of particle breakage and a linear model is  
180 therefore likely to overestimate the shear strength at higher confining pressures as well.

181 A non-linear failure envelope in the form of a power function (Equation 2b) is  
182 proposed to better describe the cohesionless shear strength of these granular CW-RC  
183 mixtures:

$$184 \quad \tau_f = \alpha \sigma_n^\beta \quad (2b)$$

185 where  $\sigma_n$  is the normal stress at failure; and  $\alpha$  and  $\beta$  are functions of rubber content

186 (Equations 2c,d):

$$187 \quad \alpha = a_1 e^{-a_2 X_{RC}} \quad (2c)$$

$$188 \quad \beta = a_3 X_{RC} + a_4 \quad (2d)$$

189 where  $a_1$ ,  $a_2$ ,  $a_3$ , and  $a_4$  are calibration parameters (Table 2) and  $X_{RC}$  is the percentage of  
190 rubber within the total mixture, defined by Equation (2e):

$$191 \quad X_{RC} = \frac{\text{Mass of RC}}{\text{Total Mass of CW-RC Mixture}} \times 100\% \quad (2e)$$

192 Therefore, mixtures with RC:CW ratios of 5%, 10%, and 15% correspond to respective  
193  $X_{RC}$  values of 4.76, 9.09, and 13.04. Figure 7 compares the calculated shear strength from  
194 this model against the measured values, as well as those from numerous studies on other  
195 granular mixtures containing rubber, which shows a coefficient of determination of,  
196  $R^2$  approaching 0.95. When extended to pure rubber (i.e.  $X_{RC} = 100$ ), the proposed  
197 model underestimates the shear strength obtained from previous studies [12,13,38],  
198 especially at lower normal stresses. This discrepancy may be attributed to the following  
199 factors:

200 **Particle breakage:** The model may not adequately encapsulate the effect CW  
201 breakage has on the shear strength of the mixture. Equation (2b) does not possess a term  
202 directly related to breakage, although it is indirectly dealt with as a result of the shear and  
203 normal stress data used in the calibration of the model. Therefore, the model may still  
204 indirectly account for CW breakage even for pure rubber and hence underestimate the  
205 shear strength as rubber would not experience breakage under these stresses due to its  
206 high compressibility and energy absorbing capacity. The investigation of a parameter  
207 incorporating particle breakage is therefore suggested to further calibrate the shear  
208 strength model for use with higher rubber contents.

209           **Cohesion of rubber:** Several studies [12,13,39] have reported non-zero cohesion  
 210 values for rubber which is an apparent cohesive-frictional material as different to  
 211 traditionally cohesionless granular materials. At low rubber contents the influence of this  
 212 inclusion is estimated to be relatively low with respect to the large portion of coal wash  
 213 within the matrix. This is in line with previous studies e.g. [40–42] which also suggested  
 214 to take the aggregate-rubber mixtures as purely frictional materials in terms of physical  
 215 mechanism contributing to strength. However, at higher rubber contents this influence  
 216 may become more significant and therefore, as the model is calibrated based on a  
 217 cohesionless mixture, the shear strength may be underestimated. Therefore, in order to be  
 218 applied to an extended range of rubber contents (including pure rubber), a parameter  
 219 relating cohesion and rubber content may need to be introduced to the model. This is a  
 220 limitation of the proposed model and requires further investigation so that the model's  
 221 accuracy is improved for mixtures with greater rubber contents.

222           Furthermore, this model is developed based on low rubber contents and it may  
 223 therefore inaccurately predict the shear behaviour at higher RC contents where the  
 224 mixture transitions to a predominately rubber-like behaviour. Consequently, a limiting  
 225 rubber content of  $RC < 60\%$  by volume is proposed as rubber-to-rubber interfaces remain  
 226 absent within the skeleton [15,21,43]. Equation (3) can be used to convert the volumetric  
 227 content of rubber within the mixture to the weight content:

$$228 \quad X_{RC} = \frac{\chi_{RC} \left( \frac{G_{s,RC}}{G_{s,CW}} \right)}{\frac{\chi_{RC}}{100} \left( \frac{G_{s,RC}}{G_{s,CW}} - 1 \right) + 1} \quad (3)$$

229 where  $\chi_{RC}$  is the percentage of RC within the total mixture by volume, and  $G_{s,RC}$  and  
 230  $G_{s,CW}$  are the specific gravities of the rubber crumbs and coal wash, respectively. The  
 231 derivation of Equation (3) is contained in the Appendix. A volumetric content of 60% RC

232 corresponds to around 40% RC by weight for these CW-RC mixtures and hence a limiting  
233 rubber content of  $X_{RC} < 40\%$  should be placed on the proposed shear strength model.

234 In view of the above, the proposed model is currently appropriate for use with the  
235 compacted CW-RC mixtures investigated in this study. For use with other waste rubber  
236 mixtures, the proposed model will require recalibration to better represent their specific  
237 shear strength response. This requirement is illustrated in Figure 7 where the model  
238 generally underestimates the strength of both SFS-CW-RC [22] and sand-tyre crumb  
239 mixtures [6]. This may be attributed to the lower particle breakage potential of these  
240 mixtures compared to CW-RC mixtures – this reasoning is discussed previously with  
241 respect to the model underestimating the strength for pure rubber.

## 242 **4. Energy Absorption Characteristics**

### 243 **4.1. Strain Energy Density**

244 The strain energy density,  $E$ , can be used to assess the strain energy absorption under  
245 triaxial shearing. It is defined as the total area under the shear stress-strain curve up to  
246 failure (Equation (4) and Figure 8 (b)).

$$247 \quad E = \int_0^{\gamma_f} \tau_f d\gamma \quad (4)$$

248 where  $E$  is the strain energy density (kPa),  $\tau_f$  is the shear strength (kPa), and  $\gamma$  and  $\gamma_f$  are  
249 the shear strain and shear strain at failure (dimensionless), respectively.

250 Figure 8 (a) presents the strain energy density of the CW-RC mixture with varying  
251 RC contents. As expected,  $E$  increases with rubber contents except for 15% RC at  $\sigma'_3 =$   
252 25 kPa. Qi et al. [22] also observed a similar response for SFS-CW-RC mixtures  
253 (mixtures of steel furnace slag (SFS), CW and RC). Noted that the most significant  
254 increase is observed for the initial addition of rubber, after which the increasing rate

255 decreases. This is most likely due to the reduction in shear strength. Referring to Figure  
256 8 (b), the pure CW has a lower strain energy density compared to that of typical subballast  
257 material and SFS-CW blends under monotonic triaxial tests conducted by Qi et al. [22].  
258 As the confining pressure increases so too does the divergence of the CW from other  
259 materials (i.e. subballast, CW-RC, and SFS-CW mixtures) which is likely attributed to  
260 the significantly higher susceptibility to particle breakage CW possesses. As reported by  
261 Indraratna et al. [20], pure CW had 13% and 46% more breakage than CW-RC mixtures  
262 with 5% RC and 15%, respectively. As breakage continues under shearing, the friction  
263 and interlocking resistance between particles may reduce and, as there is less particle  
264 movement, the CW experiences shear failure at a lower strain compared to other materials  
265 that experience less breakage. In other words, there is less time taken for the CW skeleton  
266 to reach its optimum particle arrangement which can result in a more abrupt failure and a  
267 stress-strain curve with less curvature compared to other materials that experience less  
268 breakage.

269         The results in Figure 8 (b) further highlights the influence that even a small  
270 amount of rubber crumb addition has on the energy absorbing capacity of these waste  
271 mixtures. Although pure CW has a much lower strain energy density (as low as 43%  
272 relative to typical subballast), there is a significant increase with the initial addition of 5%  
273 RC such that the CW-RC mixture is comparable to other materials without rubber (i.e.,  
274 SFS-CW mixture and typical subballast) at low confining pressures ( $\sigma'_3 \leq 25$  kPa).  
275 Although, at these low confining pressures the increase in  $E$  between the mixtures having  
276 differing RC contents is marginal. This trend was also observed with SFS-CW-RC  
277 mixtures by Qi et al. [22]. Typical railway conditions in Australia have confining  
278 pressures within this relatively low range and therefore the preferable RC content for CW-

279 RC mixtures, whether it be 5 or 15%, makes little difference for enhancing the material's  
280 strain energy absorbing potential for smaller axle loads.

281 Future developments within the industry may require trains to travel at higher  
282 speeds with heavier axle loads, meaning the applied pressures on the track will need to  
283 be increased if this is the case [44]. Therefore, increased layer thicknesses or other  
284 methods may need to be employed in order to increase the confining pressure on the  
285 substructure [45,45]. However, under larger confining pressures, these mixtures do not  
286 perform as well. At  $\sigma'_3 = 50$  kPa, only a rubber content of 15% observes an increase in  
287 strain energy density relative to typical subballast, with 10% RC resulting in a value  
288 around the same. So, it seems that the CW-RC mixtures are more appropriate for these  
289 typically lower confining pressures with respect to an increase in energy absorption  
290 relative to typical subballast material. This may be attributed to the increase in particle  
291 breakage of CW under larger confining pressures. The strain energy density of the  
292 individual CW material is significantly lower than that of subballast for these larger  
293 confining pressures ( $\sigma'_3 \geq 50$  kPa). This is illustrated in Figure 8 where subballast has a  
294 relatively constant increase in  $E$  with respect to confining pressure whereas CW  
295 experiences a diminishing increase and plateaus out. Although, typical stress ratios of  
296  $\sigma'_1/\sigma'_3$  between 3 and 4 are experienced at the subballast layer [47], corresponding to a  
297 ratio of  $q/\sigma'_3$  between 2 and 3. Figure 9 shows a similar trend with a clear improvement  
298 in strain energy density (calculated up to  $q = 2\sigma'_3$ ) for the higher confining pressures.  
299 The data shows that the role of RC is more prominent at larger loads, thus having an  
300 optimal RC of 10% will be of practical relevance for heavy haul tracks.

301 Moreover, typical track loading in the field is dynamic and cyclic in nature unlike  
302 the static loading conditions for the monotonic triaxial tests which this study is based on.  
303 Furthermore, the track is typically granted a rest period between loading cycles – i.e., the

304 time between successive trains passing over the same track section. Under static loading,  
305 the rubber particles are unable to recover the elastic portion of their deformation due to  
306 the constant and increasing nature of loading. For example, Tawk et al. [48] observed a  
307 greater energy absorption of CW-RC mixtures under cyclic loading when a rest period  
308 was introduced. As a result, the energy absorbing capabilities of these waste mixtures  
309 cannot be fully extrapolated in the context of rail applications. Nevertheless, the improved  
310 strain energy absorption (and REAP discussed in the following section) with rubber  
311 crumb content due to its elasticity and ductility is clearly evident.

#### 312 **4.2. Representative Energy Absorbing Parameter**

313 The representative energy absorbing parameter, or REAP, is a dimensionless index  
314 introduced herein as the ratio of the strain energy density of the CW-RC mixture  
315 ( $E_{CW-RC}$ ) to the pure CW ( $E_{CW}$ ):

$$316 \quad REAP = \frac{E_{CW-RC}}{E_{CW}} \quad (5)$$

317 In other words, it is a measure of the increase in strain energy density normalised to the  
318 material without rubber. Figure 10 illustrates the REAP values obtained from the triaxial  
319 testing. It is interesting to note that the tests at  $\sigma'_3 = 10$  kPa yielded the highest REAP  
320 values, a trend also observed for SFS-CW-RC mixtures as reported by Qi et al. [22]. This  
321 is likely a result of the steep shear stress-strain curve and smaller shear strain at failure  
322 for 100% CW at  $\sigma'_3 = 10$  kPa, hence a relatively low value of  $E_{CW}$ .

323 Referring to earlier Figure 5 where a RC content of up to 10% possessed a friction  
324 angle exceeding that of typical subballast, this corresponds to a REAP of 1.79 at a  
325 confining pressure of 25 kPa. In other words, the CW-RC mixtures can have an increase  
326 in strain energy density of 79% relative to the pure CW material under typical subballast

327 confinement conditions until the friction angle becomes inadequate. When normalised to  
328 the strain energy density of typical subballast material, this increase is 43% under the  
329 same confining pressure of 25 kPa.

### 330 **4.3. Empirical Relationship for Strain Energy Density**

331 From Figure 11 (a), a quasilinear trend between the strain energy density and shear  
332 strength is observed in the form of Equation (6a):

$$333 \quad E = \psi \tau_f \quad (6a)$$

334 where  $\psi$  is an empirical parameter to account for the curvature of the stress-strain  
335 response, and is a function of rubber content, depicted in Figure 11 (b) and Equation (6b):

$$336 \quad \psi = a_5 X_{RC} + a_6 \quad (6b)$$

337 where  $a_5$  and  $a_6$  are calibration parameters (Table 2). Although Equation (6a) appears to  
338 be linear, it is a function of the shear strength and hence, through Equation (2b), the strain  
339 energy density possesses a non-linear relationship with rubber content. This is an  
340 expected result and is consolidated by Figure 8 (b) where the most significant increase in  
341  $E$  is observed for the initial addition of rubber, after which the relative increase diminishes  
342 with further rubber addition. A comparison between the strain energy density calculated  
343 by Equation (6a), additionally incorporating the shear strength model from Equation (2b),  
344 and the measured values are presented in Figure 12 where a good agreement can be  
345 observed ( $R^2 = 0.98$ ). The strain energy density model is tested against an external  
346 dataset with SFS-CW-RC [22] for validation purposes (Figure 13). The model achieved  
347 a reasonable level of accuracy ( $R^2 = 0.86$ ), although different values for  $a_5$  and  $a_6$  are  
348 better suited for these different mixtures due to their differing stress-strain response.

349 Therefore, for use with other mixtures containing waste rubber inclusion, the  
350 parameters in this model should be recalibrated to better represent the specific mixture.  
351 Additionally, further investigation on the validity of this model for mixtures with higher  
352 rubber contents is required and therefore should be limited to 15% by weight at present.

## 353 5. Conclusions

354 In this study, rubber crumbs were blended with coal wash and compacted to the same  
355 initial void ratio. Triaxial tests conducted on four different CW-RC mixtures under  
356 different effective pressures were examined in terms of their ductility, shear resistance,  
357 and strain energy absorption. The following conclusions can be drawn:

358 (1) As RC contents increased, the mixtures reduced in stiffness and transitioned from  
359 a predominantly brittle to a more ductile post-peak state, with the most significant  
360 decrease occurring for the initial addition of rubber. Although the peak strength  
361 reduced with rubber content, the residual strength remained fairly consistent  
362 between the various mixtures, with a range of 44 – 50 kPa and 69 – 89 kPa for  
363  $\sigma'_3 = 10$  kPa and 25 kPa, respectively.

364 (2) The brittleness index was used as a measure to evaluate ductility and was at a  
365 minimum for the mixtures containing 10% RC at all four confining pressures  
366 tested, with the lowest value being  $I_B = 0.62$  at  $\sigma'_3 = 50$  kPa. At confining  
367 pressures  $\leq 25$  kPa, all CW-RC mixtures possess a lower brittleness index when  
368 compared to typical subballast aggregates. Similarly, mixtures with 10% and 15%  
369 rubber crumb content outperform the typical subballast with respect to  $I_B$  for all  
370 confining pressures tested.

- 371 (3) The most significant increase in strain energy density was observed for the initial  
372 inclusion of rubber, with an increase of up to 100% (i.e., doubled) at  $\sigma'_3 = 10$  kPa  
373 when compared to the pure CW material. Further improvements at higher RC  
374 contents were less significant at low confining pressures ( $\leq 25$  kPa). When  
375 evaluated at typical stress ratios experienced at the subballast layer, the strain  
376 energy density of the mixtures with 10% RC improved by 122–171% compared  
377 to the pure CW material.
- 378 (4) The internal friction angle of the mixtures was greater than that of typical  
379 subballast ( $41.6^\circ$ ) for RC contents up to 10%, allowing for a 79% and 43%  
380 increase in strain energy density relative to the pure CW and typical subballast  
381 material, respectively, under typical Australian track conditions.
- 382 (5) Empirical models developed to estimate the shear strength and strain energy  
383 density of the waste mixtures based on rubber content were in good agreement  
384 with the experimental results within this study. The shear strength model  
385 generally underestimated the measured values with an  $R^2$  value of 0.94 and is  
386 therefore more suited for use as a lower bound validation. However, the model  
387 grossly underestimated the shear strength of pure rubber and therefore a limiting  
388 RC content of 40%, corresponding to the point where the material transitions to a  
389 rubber-like behaviour, is suggested. Furthermore, as these are only empirical and  
390 rely on several empirical constants, further recalibration of these equations should  
391 be assessed when investigating other mixtures containing rubber crumbs.
- 392 (6) Overall, the inclusion of granulated rubber crumbs significantly improves the  
393 ductility and energy absorbing capabilities of coal wash, particularly for rubber  
394 contents up to 10% by weight. Although, under typical track conditions, loading  
395 is dynamic and cyclic in nature, with rest periods allowing for recovery of elastic

396 deformation. Therefore, the improved strain energy absorption of CW-RC  
 397 mixtures in this study should only be used in support of studies incorporating  
 398 cyclic loading to assess their suitability as an energy absorbing subballast layer.

### 399 **Acknowledgements**

400 The authors would like to acknowledge the financial support provided by the Australian Research  
 401 Council Linkage Project (ARC-LP200200915) and ARC Industry Transformation Training  
 402 Centre for Advanced Rail Track Technologies (ARC-ITTC-Rail). The financial and technical  
 403 assistance provided by various industry partners over the years including Australasian Centre for  
 404 Rail Innovation (ACRI), RMS and Sydney Trains, c/o Transport for NSW, SMEC, Bestech,  
 405 Douglas Partners, ASMS, South 32, Ecoflex Australia, Bridgestone, and Tyre Crumbs Australia)  
 406 is gratefully acknowledged.

### 407 **Notation**

408	CW	coal wash
409	RC	rubber crumbs
410	REAP	representative energy absorbing parameter
411	SFS	steel furnace slag
412	$E$	strain energy density (kPa)
413	$E_{CW}$	strain energy density of pure coal wash (kPa)
414	$E_{CW-RC}$	strain energy density of coal wash-rubber crumb mixtures (kPa)
415	$G_{s,CW}$	specific gravity of coal wash
416	$G_{s,RC}$	specific gravity of rubber crumbs
417	$G_{s,mix}$	specific gravity of mixture
418	$M_{RC}$	mass of rubber crumbs
419	$M_{mix}$	mass of mixture
420	$\rho_{RC}$	density of rubber crumbs
421	$\rho_{mix}$	density of mixture
422	$q$	deviator stress (kPa)
423	$q_{peak}$	peak deviator stress (kPa)
424	$q_{residual}$	residual deviator stress
425	$V_{RC}$	volume of rubber crumbs
426	$V_{mix}$	volume of mixture
427	$X_{RC}$	rubber crumb fraction of total waste mixture by weight (%)
428	$\chi_{RC}$	rubber crumb fraction of total waste mixture by volume (%)
429	$\varepsilon_1$	axial strain (major principle strain) (%)
430	$\gamma$	shear strain (%)
431	$\gamma_f$	shear strain at failure (%)
432	$\sigma'_1$	major principle stress (kPa)

433	$\sigma'_3$	effective confining pressure (minor principle stress) (kPa)
434	$\tau$	shear stress (kPa)
435	$\tau_f$	shear strength (kPa)
436	$\phi'$	internal friction angle (°)
437	$\phi'_{peak}$	peak friction angle (°)

438 **Data availability statement**

439 The data that support the findings of this study are available from the corresponding author,  
440 [B.I.], upon reasonable request.

441 **References**

- 442 [1] Leventhal A, De Ambrosis L. Waste disposal in coal mining – a geotechnical  
443 analysis. *Eng. Geol.* 1985;22(1):83–96.
- 444 [2] Waste Management Review. A rubbery problem – the Australian scrap tyre  
445 management challenge [internet]. 2016 Aug 02 [cited 2019 Aug 05]. Available  
446 from: <http://wastemanagementreview.com.au/a-rubbery-problem/>.
- 447 [3] Chiaro G, Indraratna B, Tasalloti, SMA, et al. Optimisation of coal wash–slag blend  
448 as a structural fill. *Proceedings of the Institution of Civil Engineers: Ground  
449 Improvement.* 2015;168(GI1):33–44.
- 450 [4] Commonwealth of Australia. Factsheet – Product stewardship for end-of-life tyres.  
451 Australia: Commonwealth of Australia; 2014.
- 452 [5] Sellasie KG, Moo-Young HK, Lloyd T. Determination of the initial exothermic  
453 reaction of shredded tyres with wire content. *Waste Manag Res.* 2004;22(5):364–  
454 370.
- 455 [6] Sheikh MN, Mashiri MS, Vinod JS, et al. Shear and compressibility behavior of  
456 sand-tire crumb mixtures. *J of Mater in Civ Eng.* 2013;25:1366-1374.
- 457 [7] New South Wales Environment Protection Authority (EPA) [Internet]. NSW: NSW  
458 EPA; 2019. Coal washery rejects levy; [cited 2019 Sep 02]. Available from:  
459 [https://www.epa.nsw.gov.au/your-environment/waste/waste-levy/coal-wash-](https://www.epa.nsw.gov.au/your-environment/waste/waste-levy/coal-wash-rejects)  
460 [rejects](https://www.epa.nsw.gov.au/your-environment/waste/waste-levy/coal-wash-rejects).
- 461 [8] Edil T, Bosscher P. Engineering properties of tyre chips and soil mixtures. *Geotech  
462 Test J.* 1994;17(4):453–464.
- 463 [9] Indraratna B, Qi Y, Heitor A. Evaluating the properties of mixtures of steel furnace  
464 slag, coal wash, and rubber crumbs used as subballast. *J Mater Civ Eng.*  
465 2018;30(1):04017251.
- 466 [10] American Society for Tests and Materials, Standard practice for use of scrap tires in  
467 civil engineering applications, ASTM D6270-08 (R2012), West Conshohocken.

- 468 [11] Heitor A, Indraratna B, Kaliboullah C, et al. Drained and undrained shearing  
469 behavior of compacted coal wash. *J Geotech Geoenviron Eng.*  
470 2016;142(5):04016006-1–04016006-10.
- 471 [12] Foose GJ, Benson CH, Bosscher PJ. Sand reinforced with shredded waste tires. *J*  
472 *Geotech Eng.* 1996;122(9):760–767.
- 473 [13] Zornberg, JG, Viratjandr C, Cabral AR. Behaviour of tire shred–sand mixtures. *Can*  
474 *Geotech J.* 2004;41(2):227–241.
- 475 [14] Mashiri M, Vinod JS, Sheikh MN, et al. Shear strength and dilatancy behaviour of  
476 sand–tyre chip mixtures. *Soil Found.* 2015;55(3):517–528.
- 477 [15] Kim H-K, Santamarina JC. Sand–rubber mixtures (large rubber chips). *Can Geotech*  
478 *J.* 2008;45(10):1457–1466.
- 479 [16] Topçu İB. Assessment of the brittleness index of rubberized concretes. *Cem Concr*  
480 *Res.* 1997;27(2):177–183.
- 481 [17] Alam I, Mahmood U A, Khattak, N. Use of rubber as aggregate in concrete: A  
482 review. *Int J Adv Struct Geotech Eng.* 2015;4(2):92–96.
- 483 [18] Hossain FMZ, Shahjalal M, Islam K, et al. Mechanical properties of recycled  
484 aggregate concrete containing crumb rubber and polypropylene fiber. *Constr*  
485 *Build Mater.* 2019;225:983–996.
- 486 [19] Aly AM, El-Feky MS, Kohail M, et al. Performance of geopolymer concrete  
487 containing recycled rubber. *Constr Build Mater.* 2019;207:136–144.
- 488 [20] Indraratna B, Rujikiatkamjorn C, Tawk M, et al. Compaction, degradation and  
489 deformation characteristics of an energy absorbing matrix. *Transp Geotech.*  
490 2019;19:74–83.
- 491 [21] Qi Y, Indraratna B, Heitor A, et al. Effect of rubber crumbs on the cyclic behavior  
492 of steel furnace slag and coal wash mixtures. *J Geotech Geoenviron Eng.*  
493 2018;144(2):04017107.
- 494 [22] Qi Y, Indraratna B, Heitor A, et al. The Influence of Rubber Crumbs on the Energy  
495 Absorbing Property of Waste Mixtures. *Proceedings of the International*  
496 *Symposium on Geotechnics of Transportation Infrastructure (ISGTI 2018); India:*  
497 *Indian Institute of Technology Delhi; 2018. p. 455–460.*
- 498 [23] Qi Y, Indraratna B, Vinod JS. Behavior of steel furnace slag, coal wash, and rubber  
499 crumb mixtures with special relevance to stress-dilatancy relation. *J Mater Civ*  
500 *Eng.* 2018;30(11):04018276.

- 501 [24] Tian Y, Senetakis K. Influence of creep on the small-strain stiffness of sand–rubber  
502 mixtures. *Geotechnique*. 2021;1-12.
- 503 [25] Cho S, Kim J-M, Kim J-H, et al. Utilization of Waste Tires to Reduce Railroad  
504 Vibration. *Mater Sci Forum*. 2007;544-545:637-640.
- 505 [26] Fernández PM, Signes CH, Sanchís IV, et al. Real scale evaluation of vibration  
506 mitigation of sub-ballast layers with added tyre-derived aggregate. *Constr Build*  
507 *Mater*. 2018;169:335–346.
- 508 [27] Jayasuriya C, Indraratna B, Ngoc Ngo T. Experimental study to examine the role of  
509 under sleeper pads for improved performance of ballast under cyclic  
510 loading. *Transp Geotech*. 2019;19:61–73.
- 511 [28] Indraratna B, Nimbalkar S, Rujikiatkamjorn C. Future of Australian rail tracks  
512 capturing higher speeds with heavier freight. In Khabbaz M, Tey C, Stahlhut O,  
513 Rujikiatkamjorn C (eds.); *Advances in Geotechnical Aspects of Roads and*  
514 *Railways*; 2012; Australia: The Australian Geomechanics Society; 2012. p. 1– 24.
- 515 [29] Australian Rail Track Corporation (ARTC). *Earthworks Materials Specification*  
516 *ETC-08-03*. Australia: Australian Rail Track Corporation Limited; 2010.
- 517 [30] Consoli N C, Prietto PDM, Ulbrich LA. (1998) ‘Influence of fiber and cement  
518 addition on behavior of sandy soil. *J Geotech Geoenv Eng*. 1998;124(12):1211.
- 519 [31] Xiao Y, Meng M, Daouadji A, et al. Effects of particle size on crushing and  
520 deformation behaviors of rockfill materials. *Geosci Front*. 2020;11(2):375–388.
- 521 [32] Qi Y, Indraratna B, Tawk M. Use of recycled rubber elements in track stabilisation.  
522 In *Geo-Congress 2020: Geo-Systems, Sustainability, Geoenvironmental*  
523 *Engineering, and Unsaturated Soil Mechanics*. 2020, February; p. 49–59. Reston,  
524 VA: American Society of Civil Engineers.
- 525 [33] Tawk M, Indraratna B. Role of rubber crumbs on the stress-strain response of a coal  
526 wash matrix. *J Mater Civ Eng*. 2021;33(3):04020480.
- 527 [34] Rujikiatkamjorn C, Indraratna B, Chiaro, G. Compaction of coal wash to optimise  
528 its utilisation as water-front reclamation fill. *Geomech Geoeng*. 2013;8(1):36–45.
- 529 [35] Leventhal A. Coal washery reject as an engineered material. In: *National Symposium*  
530 *on the Use of Recycled Materials in Engineering Construction (1st: 1996: Sydney,*  
531 *NSW)*. National Symposium on the Use of Recycled Materials in Engineering  
532 *Construction: 1996; Programme & Proceedings*; Barton, ACT: Institution of  
533 *Engineers, Australia*; 1996. p. 54–59.

- 534 [36] Tasalloti SMA, Indraratna B, Rujikiatkamjorn C, et al. A laboratory study on the  
535 shear behaviour of mixtures of coal wash and steel furnace slag as potential  
536 structural fill. *Geotech Test J.* 2015;38(4):361–372.
- 537 [37] Heitor A, Indraratna B, Rujikiatkamjorn C, et al. Evaluation of the coal wash and  
538 steel furnace slag blends as effective reclamation fill for port expansion.  
539 Proceedings of the 7th International Congress on Environmental Geotechnics,  
540 Bouazza A, Yuan STS, Brown B (eds.); 2014 November 10–14; Melbourne,  
541 Australia: Engineers Australia; 2014. p. 972–979.
- 542 [38] Marto A, Latifi N, Moradi R, et al. Shear properties of sand – tire chips mixtures,  
543 *Electron J Geotech Eng.* 2013;18.
- 544 [39] Humphrey D, Sandford T, Cribbs M, et al. Shear strength and compressibility of tire  
545 chips for use as retaining wall backfill. *Transp Res Rec.* 1993;1422:29–35.
- 546 [40] Li W, Kwok CY, Sandeep CS, et al. Sand type effect on the behaviour of sand-  
547 granulated rubber mixtures: Integrated study from micro-to macro-scales. *Powder*  
548 *Technol.* 2019;342:907–916.
- 549 [41] Li W, Kwok CY, Senetakis K. Effects of inclusion of granulated rubber tires on the  
550 mechanical behaviour of a compressive sand. *Can Geotech J.* 2020;57(5):763–  
551 769.
- 552 [42] Tian Y, Senetakis K. On the contact problem of soft-rigid interfaces: incorporation  
553 of Mindlin-Deresiewicz and self-deformation concepts. *Granul Matter.*  
554 2022;24(1):1–17.
- 555 [43] Senetakis K, Anastasiadis A, Pitilakis K. Dynamic properties of dry sand/rubber  
556 (SRM) and gravel/rubber (GRM) mixtures in a wide range of shearing strain  
557 amplitudes. *J Soil Dyn Earthq Eng.* 2012;33(1):38–53.
- 558 [44] Indraratna B, Sun Q, Grant J. Behaviour of subballast reinforced with used tyre and  
559 potential application in rail tracks. *Transp Geotech.* 2017;12:26–36.
- 560 [45] Indraratna B, Salim W, Rujikiatkamjorn C. *Advanced rail geotechnology – ballasted*  
561 *track.* London: CRC Press; 2011.
- 562 [46] Indraratna B, Biabani MM, Nimbalkar S. Behavior of geocell-reinforced subballast  
563 subjected to cyclic loading in plane-strain condition. *J Geotech Geoenviron Eng.*  
564 2014;141(1):04014081.
- 565 [47] Signes CH, Fernández PM, Garzón-Roca J, et al. An evaluation of the resilient  
566 modulus and permanent deformation of unbound mixtures of granular materials

567 and rubber particles from scrap tyres to be used in subballast layers. *Transp Res*  
568 *Proc.* 2016;18:384–391.

569 [48] Tawk M, Qi Y, Indraratna B, et al. Behaviour of a mixture of coal wash and rubber  
570 crumbs under cyclic loading. *J Mater Civ Eng.* 2021;33(5):04021054.

571

572

573 **Appendix**

574 *Derivation of volume fraction to mass fraction of rubber crumb content*  
575 *conversion*

576 The mass fraction of RC within the total mixture,  $X_{RC}$ , is defined as:

577 
$$X_{RC} (\%) = \frac{M_{RC}}{M_{mix}} \times 100 \quad (A1)$$

578 where  $M_{RC}$  and  $M_{mix}$  are the masses of the rubber crumbs and the total mixture,  
579 respectively.

580 Similarly, the volumetric fraction of RC within the total mixture,  $\chi_{RC}$ , is defined as:

581 
$$\chi_{RC} (\%) = \frac{V_{RC}}{V_{mix}} \times 100 \quad (A2)$$

582 where  $V_{RC}$  and  $V_{mix}$  are the volumes of the rubber crumbs and the total mixture,  
583 respectively.

584 By definition,

585 
$$M_{RC} = V_{RC} \rho_{RC} \quad (A3)$$

586 
$$M_{mix} = V_{mix} \rho_{mix} \quad (A4)$$

587 where  $\rho_{RC}$  and  $\rho_{mix}$  are the densities of the rubber crumbs and the mixture, respectively.

588 Therefore, Equation (A1) can be rewritten as:

589 
$$X_{RC} (\%) = \frac{V_{RC}}{V_{mix}} \frac{\rho_{RC}}{\rho_{mix}} \times 100 \quad (A5)$$

590 From Equation (A2), Equation (A5) can be rewritten as:

591 
$$X_{RC} (\%) = \chi_{RC} \frac{\rho_{RC}}{\rho_{mix}} \quad (A6)$$

592 However, the ratio of the densities may also be expressed as an equivalent ratio of the  
593 specific gravities:

594 
$$\frac{\rho_{RC}}{\rho_{mix}} = \frac{G_{s,RC}}{G_{s,mix}} \quad (A7)$$

595 where  $G_{s,RC}$  and  $G_{s,mix}$  are the specific gravities of the rubber crumbs and mixture.

596 Adapted from Indraratna et al. [20], the specific gravity of the mixture may be expressed  
597 as:

598 
$$G_{s,mix} = \frac{1}{\frac{\chi_{RC}}{G_{s,RC}} + \frac{100-\chi_{RC}}{G_{s,CW}}} \quad (A8)$$

599 where  $G_{s,CW}$  is the specific gravity of coal wash.

600 Therefore, the mass fraction of the rubber crumbs within the mixture may be calculated  
601 as:

602 
$$X_{RC} (\%) = \frac{\chi_{RC} \left( \frac{G_{s,RC}}{G_{s,CW}} \right)}{\frac{\chi_{RC}}{100} \left( \frac{G_{s,RC}}{G_{s,CW}} - 1 \right) + 1} \quad (A9)$$

603 Noted that a volumetric RC content of 60% corresponds to  $\chi_{RC} = 60$  in the above  
604 equation.

605 Table 1. Shear strength and strain energy density of CW-RC mixtures from monotonic  
 606 triaxial tests

$\sigma'_3$ (kPa)	RC:CW (%)	$X_{RC}$ (%)	$\tau_f$ (kPa)	$\phi'_{peak}$ (°)	$\phi'$ (°)	$E$ (kPa)
10	0	0	33.7	61.0	45.0	0.67
	5	4.76	28.6	57.2	44.3	1.34
	10	9.09	25.4	54.5	42.0	1.73
25	0	0	62.8	54.2	45.0	2.16
	5	4.76	57.3	52.0	44.3	3.28
	10	9.09	50.5	49.0	42.0	3.87
	15	13.04	45.5	46.5	40.6	3.83
50	0	0	107.4	50.5	45.0	2.91
	5	4.76	99.2	48.6	44.3	4.63
	10	9.09	92.7	47.0	42.0	5.67
	15	13.04	82.0	44.1	40.6	6.72
75	0	0	144.3	47.9	45.0	3.95
	5	4.76	143.2	47.7	44.3	6.33
	10	9.09	124.6	44.4	42.0	7.28
	15	13.04	120.9	43.6	40.6	8.62

607

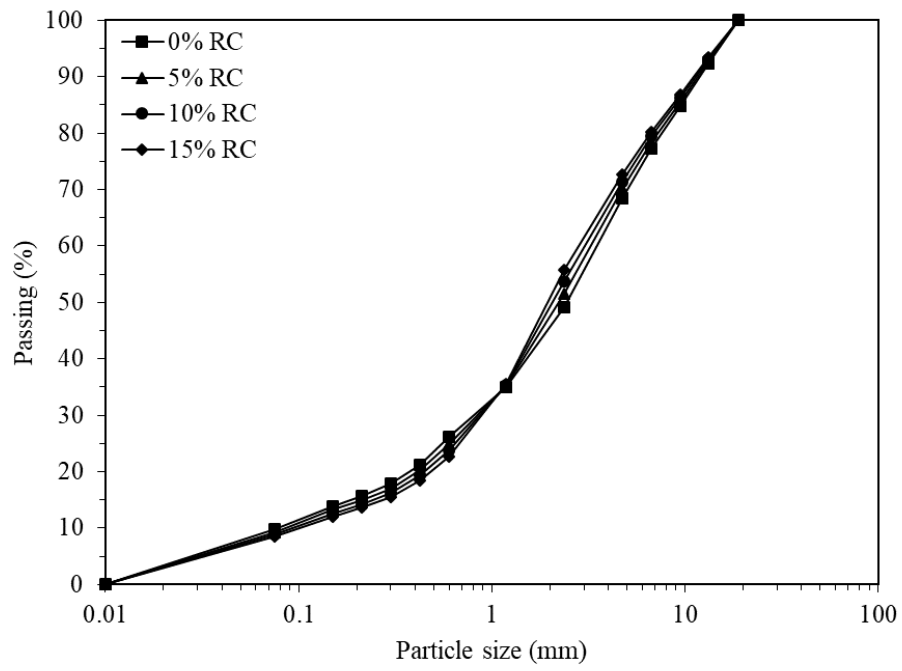
608 Table 2. Calibration parameters for shear strength and strain energy density models

Source	Parameter	Value
Shear strength Eq. 2(c-d)	$a_1$	3.6986
	$a_2$	0.064
	$a_3$	0.0106
	$a_4$	0.7529
Strain energy density, Eq. 6b	$a_5$	0.0036
	$a_6$	0.0282

609

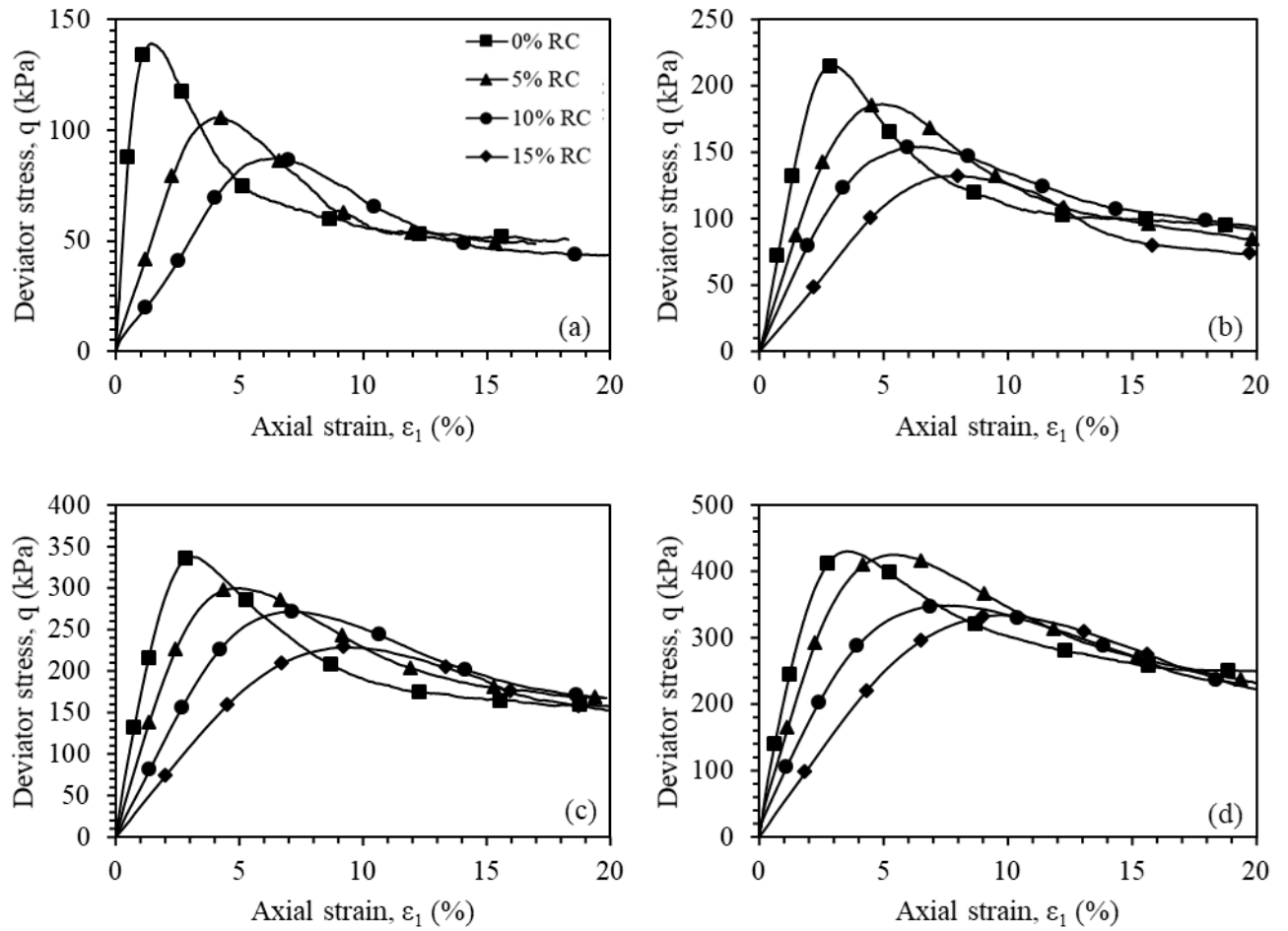
610 **List of Figures**

- 611 Figure 1. Particle size distribution of CW-RC mixtures with varying rubber content
- 612 Figure 2. Stress-strain curves of CW-RC mixtures at effective confining pressures of (a)  
613 10 kPa; (b) 25 kPa; (c) 50 kPa; (d) 75 kPa (Modified after Indraratna et al. [20])
- 614 Figure 3. Volume change behaviour of CW-RC mixtures with varying rubber content and  
615 effective confining pressures (Modified after Indraratna et al. [20])
- 616 Figure 4. Brittleness index of CW-RC mixtures with respect to (a) RC content and (b)  
617 confining pressure compared to typical subballast
- 618 Figure 5. Internal friction angle of CW-RC mixtures at varying RC contents compared to  
619 typical subballast
- 620 Figure 6. Mohr circles with non-linear and linear failure envelope for CW-RC mixture  
621 with 10% RC
- 622 Figure 7. Predicted shear strength comparing with measured data from current study and  
623 previous studies
- 624 Figure 8. Strain energy density of CW-RC mixtures (a) under varying confining pressure;  
625 and (b) in comparison to typical subballast and steel furnace slag-coal wash waste mixture  
626 with definition of strain energy density
- 627 Figure 9. Strain energy density of CW-RC mixtures at a stress ratio of  $q = 2\sigma'_3$  typically  
628 experienced at the subballast layer
- 629 Figure 10. REAP indices for CW-RC mixtures
- 630 Figure 11. (a) Increase in strain energy density with respect to shear strength at varying  
631 rubber content; and (b) calibration parameter  $\psi$  as a linear function of rubber content for  
632 strain energy density model
- 633 Figure 12. Comparison between calculated strain energy densities incorporating shear  
634 strength and strain energy density models with respect to measured values
- 635 Figure 13. Validation of strain energy density model using external SFS-CW-RC data



636

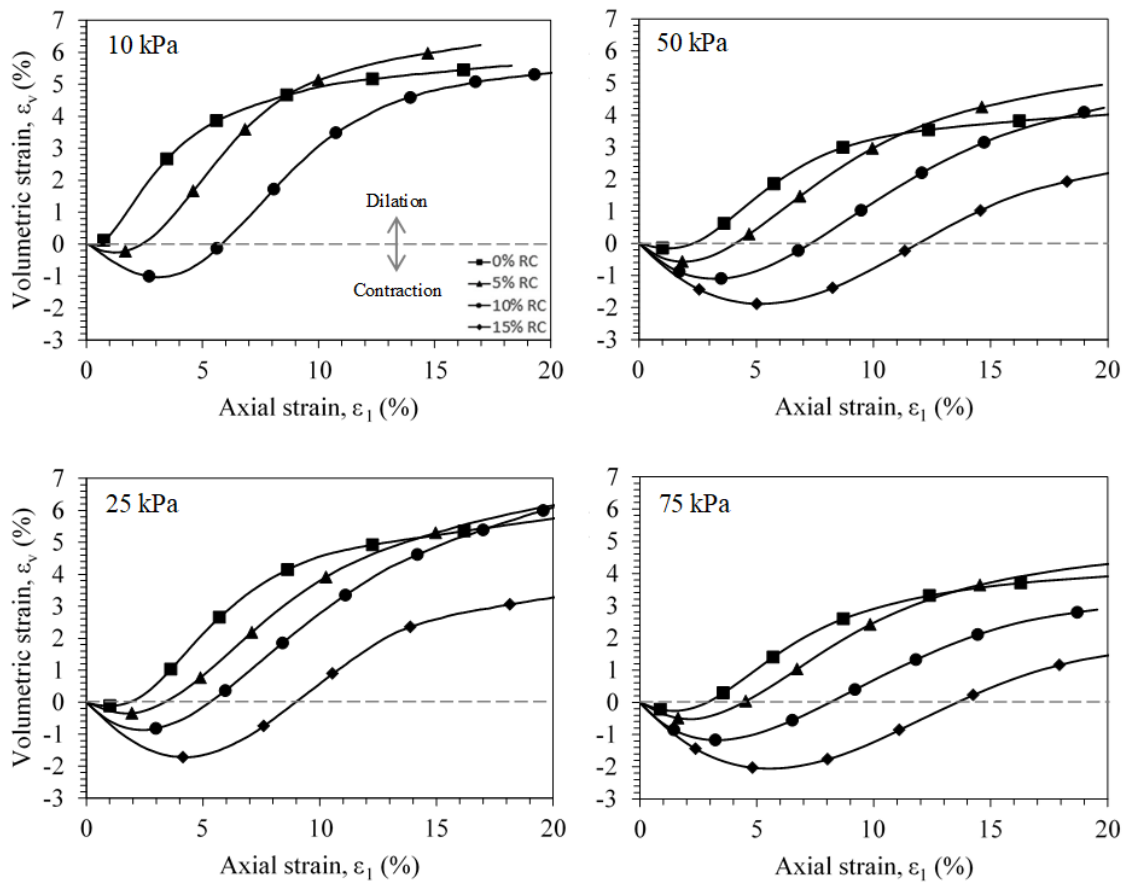
637 Figure 1. Particle size distribution of CW-RC mixtures with varying rubber content



638

639 Figure 2. Stress-strain curves of CW-RC mixtures at effective confining pressures of (a)  
 640 10 kPa; (b) 25 kPa; (c) 50 kPa; (d) 75 kPa (Modified after Indraratna et al. [20])

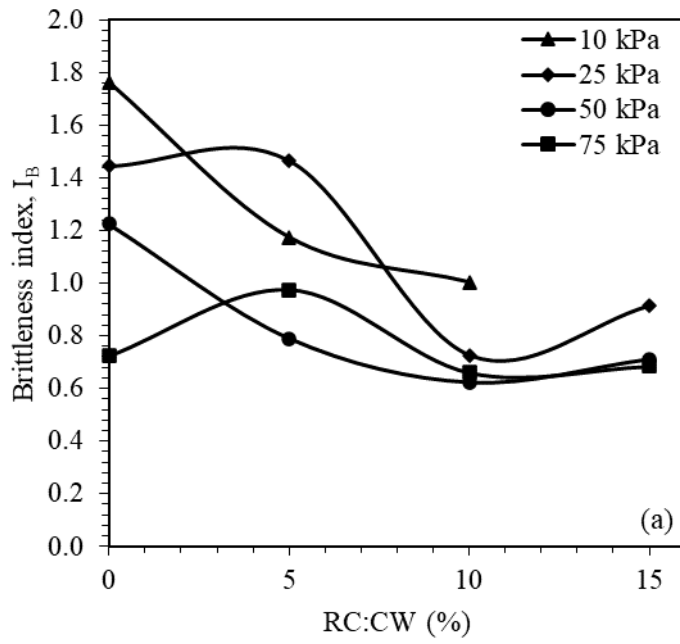
641



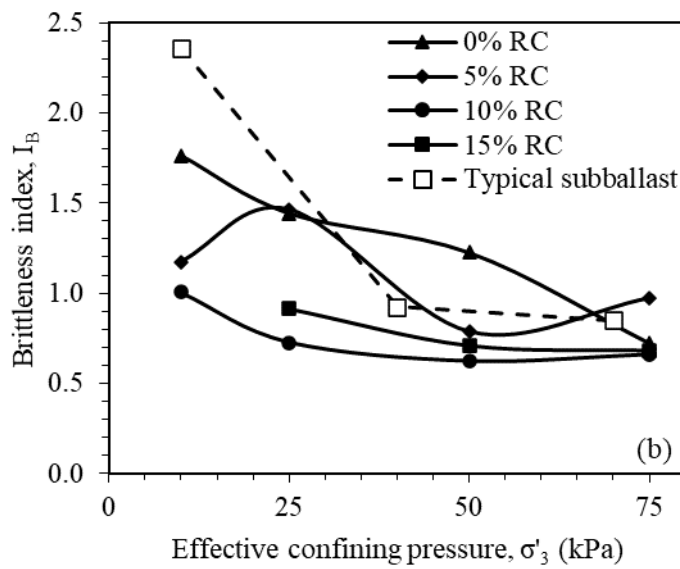
642

643 Figure 3. Volume change behaviour of CW-RC mixtures with varying rubber content and

644 effective confining pressures (Modified after Indraratna et al. [20])

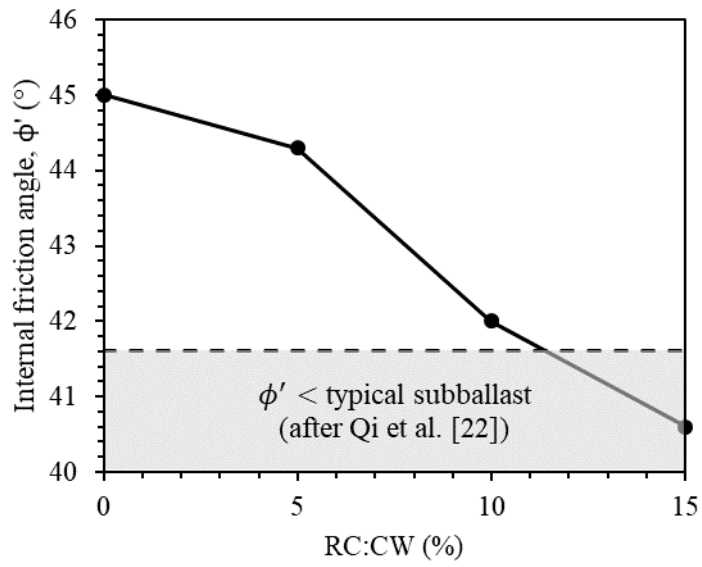


645



646

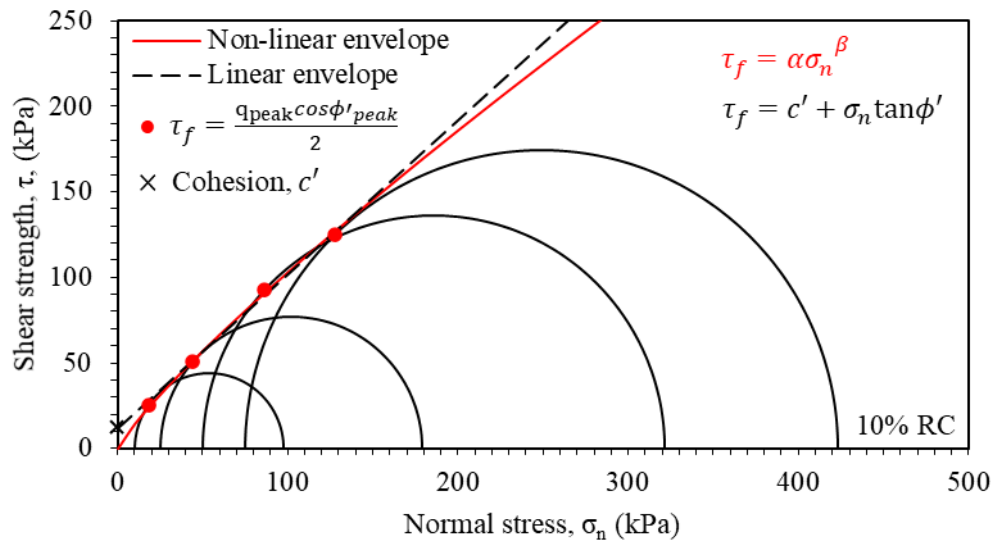
647 Figure 4. Brittleness index of CW-RC mixtures with respect to (a) RC content and (b)  
 648 confining pressure compared to typical subballast



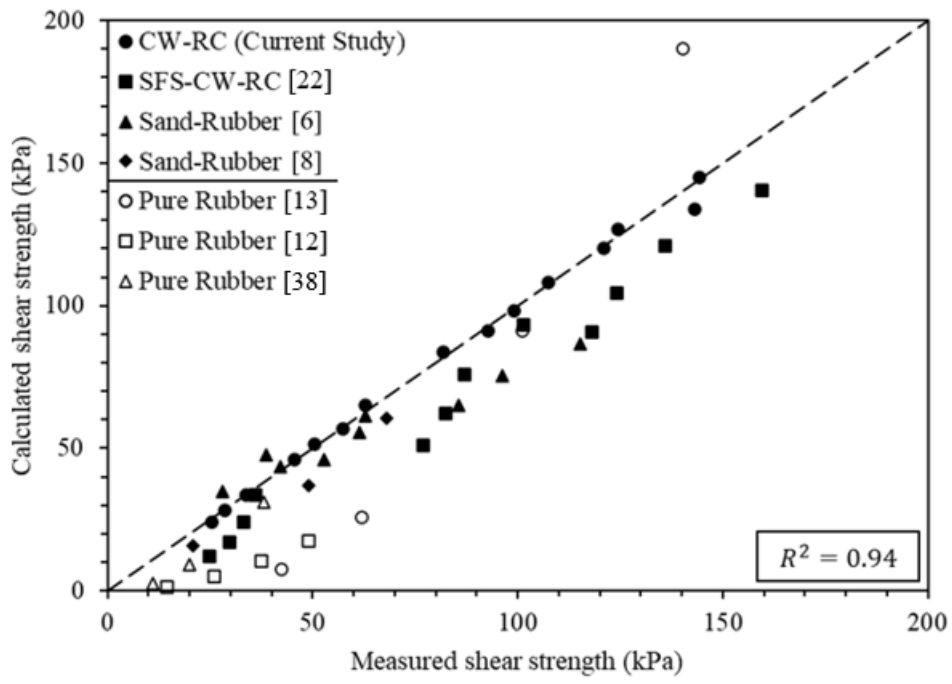
649

650 Figure 5. Internal friction angle of CW-RC mixtures at varying RC contents compared to  
 651 typical subballast

652



661 Figure 6. Mohr circles with non-linear and linear failure envelope for CW-RC mixture  
 662 with 10% RC  
 663

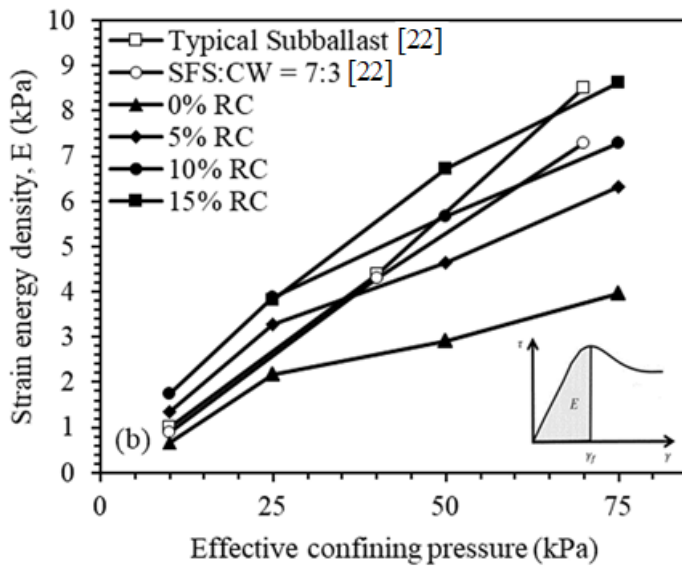
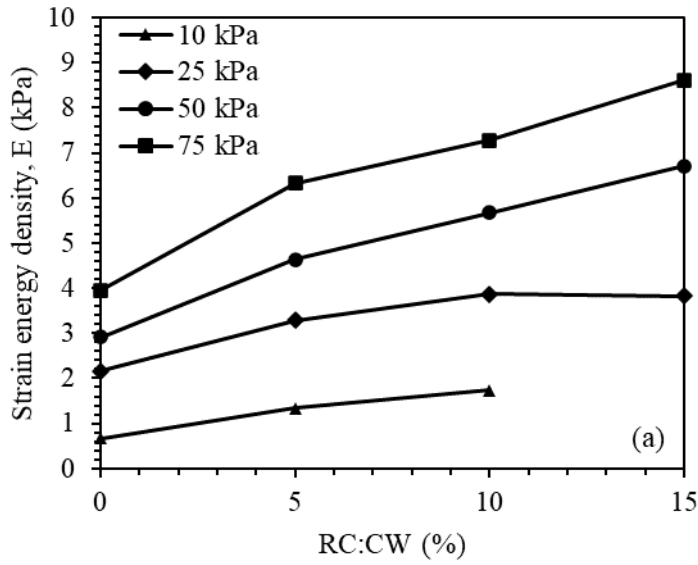


0/3

674 Figure 7. Predicted shear strength comparing with measured data from current study and  
 675 previous studies

676

677

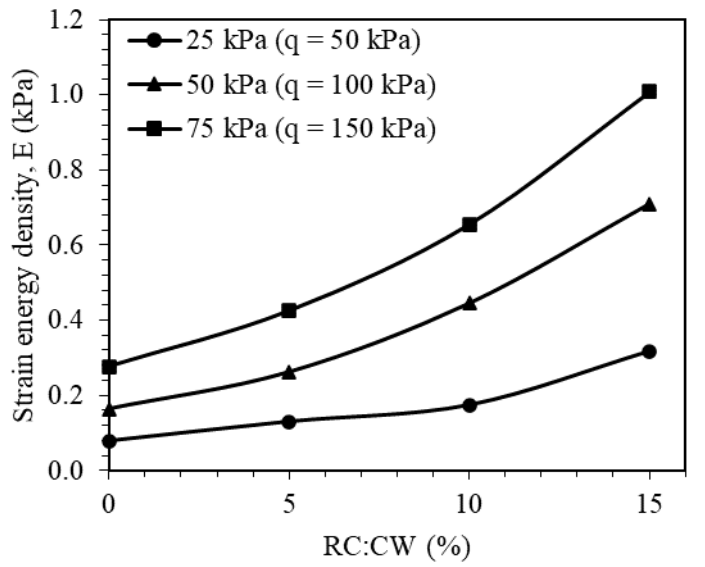


686

687 Figure 8. Strain energy density of CW-RC mixtures (a) under varying confining pressure;  
 688 and (b) in comparison to typical subballast and steel furnace slag-coal wash waste mixture  
 689 with definition of strain energy density

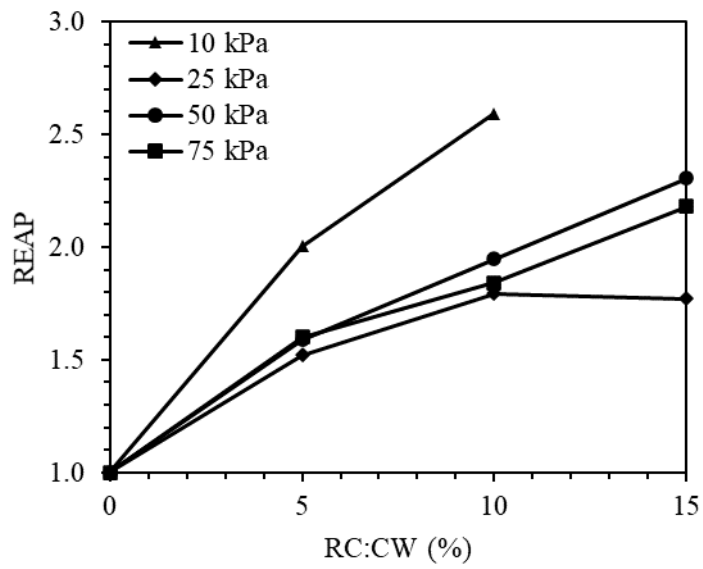
690

691



700

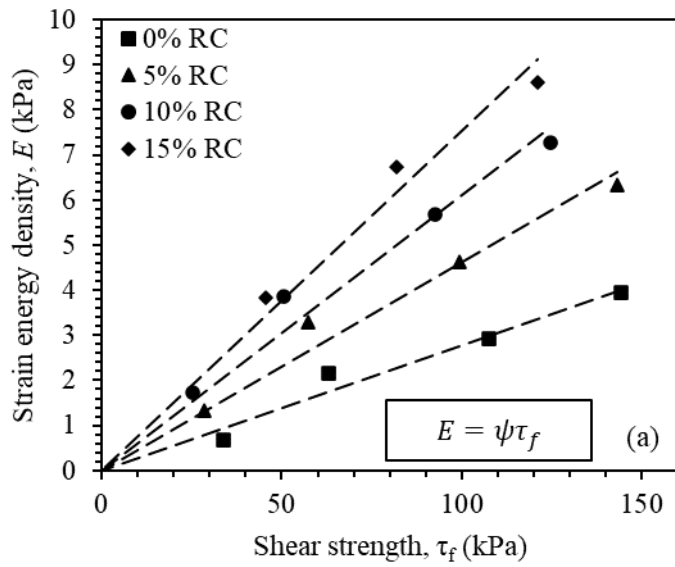
701 Figure 9. Strain energy density of CW-RC mixtures at a stress ratio of  $q = 2\sigma'_3$  typically  
 702 experienced at the subballast layer  
 703



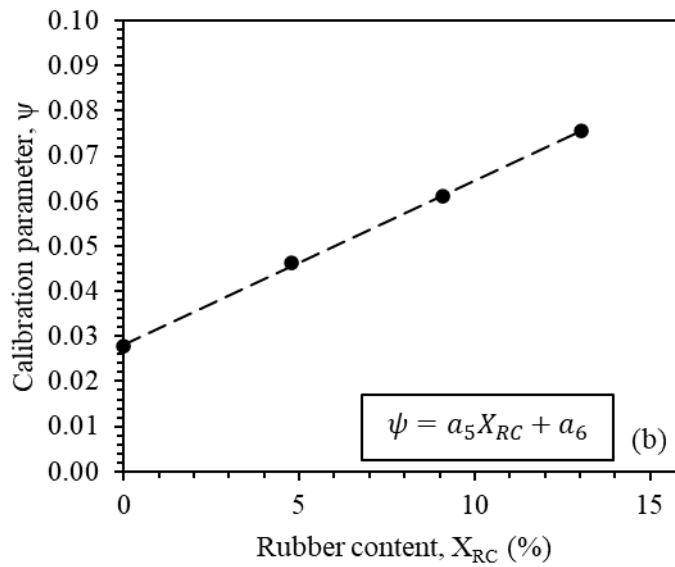
704

705 Figure 10. REAP indices for CW-RC mixtures

706



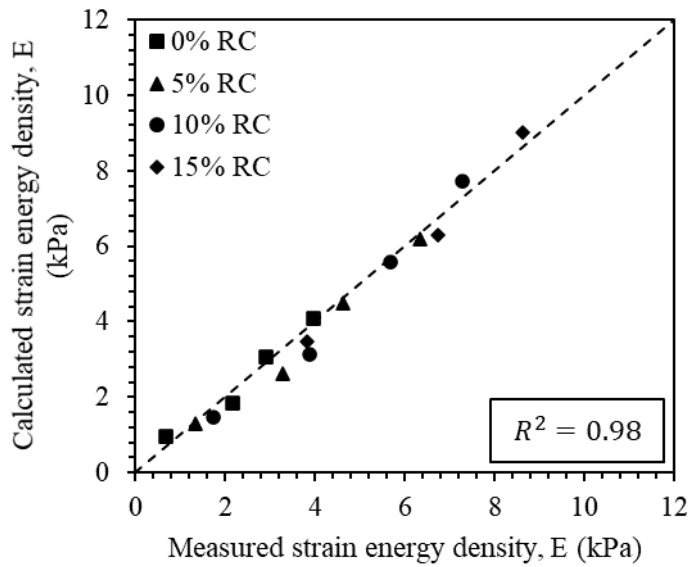
707



708

709 Figure 11. (a) Increase in strain energy density with respect to shear strength at varying  
 710 rubber content; and (b) calibration parameter  $\psi$  as a linear function of rubber content for  
 711 strain energy density model

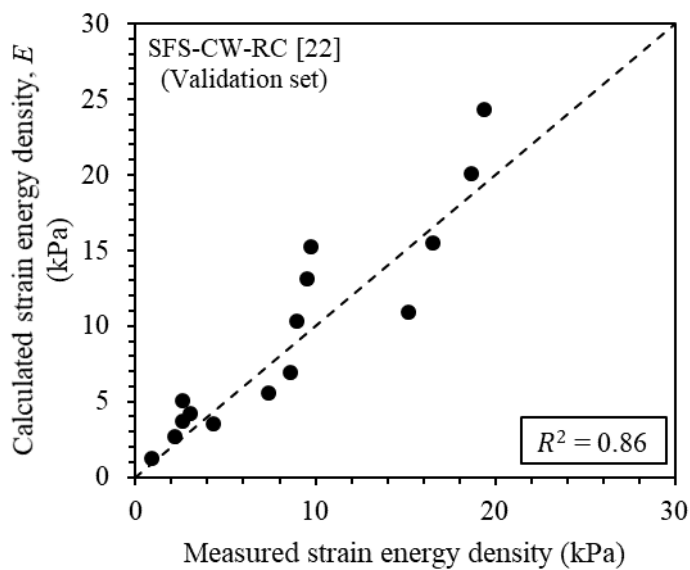
712



713

714 Figure 12. Comparison between calculated strain energy densities incorporating shear  
 715 strength and strain energy density models with respect to measured values

716



717

718 Figure 13. Validation of strain energy density model using external SFS-CW-RC data